

# Development of ZnO thin films for Dye-Sensitized Solar Cells applications

---

Submitted By

Joydeep Das

In partial Fulfillment for the award of the degree of

**MASTER OF SCIENCE**

**IN**

**PHYSICS**

UNDER THE ESTEEMED GUIDANCE OF

**Dr. Sai Santosh Kumar Raavi**



भारतीय प्रौद्योगिकी संस्थान हैदराबाद  
Indian Institute of Technology Hyderabad

**DEPARTMENT OF PHYSICS**

**INDIAN INSTITUTE OF TECHNOLOGY HYDERABAD**

**KANDI, SANGAREDDY, TELANGANA-502285**

## Approval Sheet

This thesis entitled –**Development of ZnO thin films for dye-sensitized solar cells applications**– by –**Joydeep Das** – is approved for the degree of Master of Science from IIT Hyderabad.

Vandana Sharma

Examiner

Dept. of Physics (IITH)

P. Bhuvanesh

Examiner

Dept. of Physics (IITH)

Dr. Sai Santosh Kumar Raavi

Dr. Sai Santosh Kumar Raavi

Adviser

Dr. Jayaraman

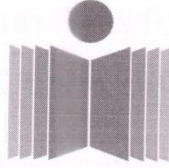
Examiner

Dept. of Physics (IITH)

Dr. M. S. Anil Kumar

Examiner

Dept. of Physics (IITH)



भारतीय प्रौद्योगिकी संस्थान हैदराबाद  
Indian Institute of Technology Hyderabad

**Indian Institute of Technology**

**Hyderabad**

**CERTIFICATE**

This is to certify that the thesis entitled “**Development of ZnO thin films for dye-sensitized solar cells applications**” is submitted by **Mr. JOYDEEP DAS**, (Roll - **PH14MSCST11006**) to this Institute in partial fulfillment of the requirement for the award of the degree of Master of Science in **Department of Physics**, is a bonafide record of the work carried out under my supervision and guidance. It is further certified that no part of this thesis is submitted for the award of any other degree.

**Hyderabad**

**Date** 28/04/2016


**Dr. Sai Santosh Kumar Raavi**

**Supervisor**

**Department Of Physics**

## Declaration

I declare that this written submission represents my ideas in my own words, and where ideas or words of others have been included, I have adequately cited and referenced the original sources. I also declare that I have adhered to all principles of academic honesty and integrity and have not misrepresented or fabricated or falsified any idea/data/fact/source in my submission. I understand that any violation of the above will be a cause for disciplinary action by the Institute and can also evoke penal action from the sources that have thus not been properly cited, or from whom proper permission has not been taken when needed.



(Signature)

(JOYDEEP DAS)  
(Roll No.-PH14MSCST11006)

## ACKNOWLEDGEMENTS

Firstly I would like to express my sincere thanks to my supervisor, **Dr. Sai Santosh Kumar Raavi**, Department of Physics, IIT Hyderabad, for his esteemed supervision, incessant support, and inspiration throughout my project work.

I accord my thanks to Dr. L Giribabu, Senior Scientist, Inorganic and Physical Chemistry Division, IICT Hyderabad for providing me the dye for the project work and also for allowing me take further readings for my solar cell.

I would like to thank Dr. Ranjith Ramdurai, Department of Material Science Engineering, for allowing me to do GI-XRD in his lab.

Also I would like to thank Dr. Suryanarayana Jammalamadaka, Department of Physics, IIT Hyderabad for allowing me to use UV Visible Spectrometer for my project work.

Also I would like to thank Dr. Jyoti Ranjan Mohanty, Department of Physics, IIT Hyderabad for allowing me to use 3D Profilometer for my project work.

I would also thank to H.O.D and all other faculty members of Department of Physics, IIT Hyderabad, for their co-operation.

I convey my thanks to Mr. A Soundaraj, Mr. Mr. K Raja Kandula, Mr. V Sai Krishna, Mr. Venkatnarayana, Miss. Aparajita, Mr. Sajmohan, Mr. Kumaraswamy Miriyala, Mr. Manmohan Sahoo, Mr. Abhisekh Talapatra (PhD Scholars) and Mr. Naresh (IICT PhD scholar) for their valuable suggestion and help.

Finally, I would also express my deep sense of gratitude to my Parents, God and Family members for their encouragement and support throughout, which always inspired me.

## **DEDICATION**

**This Work is dedicated to My Parents and Relatives.**

CONTENTS:

I.APPROVAL SHEET	2
II.CERTIFICATE	3
III.DECLARATION	4
IV.ACKNOWLEDGEMENT	5
1. INTRODUCTION AND MOTIVATION	8
2. ZnO –AN INTRODUCTION	10
3. SYNTHESIS	13
I.SYNTHESIS OF ZnO-1	
II.SYNTHESIS OF ZnO-2	
4. CHARACTERISATION	
I.UV Vis. SPECTROSCOPIC ANALYSIS	16
II.GIXRD	25
III.OPTICAL PROFILOMETER ANALYSIS	29
5. WORK ON SOLAR CELL	34
5.1G1 AND DYE G1 INTERFACE	
5.2 PREPARATION OF ZnO AND DYE G1 INTERFACE	
5.3 EXPERIMENTAL SET UP	
5.4RESULTS AND DISCUSSION	
6. VARIOUS PARAMETERS IN SOLAR CELL	43
7. CONCLUSION	47
8.REFERENCES	48

## ABSTRACT:

In my present work, thin films of ZnO are optimized for DSSC operation. ZnO nanoparticles were prepared by sol gel method using two different solvents(Ethanol and 2MEA) while the precursor was the same Zinc Acetate Dihydrate. Then this sol was used to prepare thin films of ZnO using spin coating method. The thickness of the multiple coated films were found out to be roughly 100nm while the roughness was measured to be around 20nm when observed using Zeta 3D Profilometer. UV Vis. Spectroscopic analysis of the samples were done using UV-3600 PLUS spectrophotometer. The analysis showed peaks at around 345nm which corresponds to the band gap of ZnO. This evidence of ZnO being deposited on the substrates was substantiated by the GIXRD patterns of the thin films which was done using Bruker D8 Discover. The XRD patterns of the samples confirmed the presence of the expected phase with little impurities. Using G1 dye, Light I-V measurement were done on the samples which helped us record a maximum  $V_{OC}$  of 612.6mV with an efficiency of 0.53%. J vs. V plots showed maximum J values for the cells with the film containing 3 coats of the sol. Photoluminescence and absorption spectroscopy were used to observe electron transfer process in G1-ZnO interface. Electron injection from G1 dye to ZnO thin films were observed. Photoluminescence spectra of dye G1 (Anthracene based organic molecule)-ZnO showed electron injection occurring at 345 and 460 nm of wavelength impinging.



## 1)Introduction And Motivation:

At the end of last century, the possibility to use devices based on molecular components for the construction of a robust large-scale solar electricity production facility seemed to be originate. But the seminal paper by O'Regan and Gratzel in 1991 spurred researchers to take on the challenge. With the development of dye-sensitized solar cells (DSCs), conventional solid-state photovoltaic technologies are now challenged by devices functioning at a molecular and nano level. The prospect of low-cost investments and fabrication are key features. DSCs perform also relatively better compared with other solar cell technologies under diffuse light conditions and at higher temperatures. DSCs offer the possibilities to design solar cells with a large flexibility in shape, color, and transparency. Here for DSCs applications we are using organic dye G1 and inorganic semiconducting material ZnO interface. We then look at the absorption and emission spectra of dye and ZnO interface. The absorption spectra are determined by the intrinsic absorption of the dye molecules and the dye – ZnO interaction. Dye-dye (solute-solute) interaction is negligible because of the large average distance between the dye molecules. The absorption spectra obey the Beer-Lambert law, i.e. the absorption cross sections are independent of concentration.

Semiconductor compounds have drawn much attention during the last few years because of their relatively new optical and transport properties which have great many potential for optoelectronic applications. ZnO is a wide band gap semiconductor that displays high optical transparency and luminescent properties in the near ultra violet and the visible regions. Due to these properties ZnO is a promising material for electronic and optoelectronic applications such as solar cells (anti-reflecting coating and transparent conducting materials), gas sensors, liquid crystal displays, heat mirrors, surface acoustic wave devices etc. The high exciton binding energy of ZnO (~ 60 meV) would allow for excitonic transitions even at room temperature, which could mean high radiative recombination efficiency for spontaneous emission as well as a lower threshold voltage for laser emission. Studies have been carried out to fine-tune the properties of ZnO to adopt it for different applications; for example, the band gap of ZnO is modified to use as UV detectors and emitters. ZnO nanoparticles are widely employed in fundamental research and potential applications, such ultraviolet lasers and diodes, piezoelectric devices and photo

catalysts fluorescence labels in medicine and biology, controlling units as UV photo detectors and as high-flame detectors in cosmetic industry and as a component of sun screens.

## **2.ZnO -AN INTRODUCTION:**

Zinc oxide shows a wide range of chemical and physical properties. It has high chemical stability, broad range of radiation absorption, high photostability and high electrochemical coupling coefficient. It is also a multifunctional material [1,2]. Zinc oxide is also classified as a semiconductor in group II-VI (because Zinc belongs to Group II and Oxygen belongs to group VI) having a covalence value on the between that of ionic and covalent semiconductors. It has a broad energy band (3.37 eV), a high bond energy (60 meV) and high thermal and mechanical stability at room temperature. Because of its all these properties, people find it useful in electronics, optoelectronics and laser technology [3,4]. ZnO also shows piezo and pyro electric properties which makes it suitable for application in sensors, converters, energy generator and photocatalyst in hydrogen production [5,6]. The hardness, rigidity and piezoelectric constant of this material make it an important material in the ceramics industry. Again because of its low toxicity, biocompatibility and good biodegradability, it finds its application in the field of biomedicine and in pro-ecological systems [7,9].

### **Structure:**

Generally II-VI binary compound semiconductors crystallize in either cubic zinc blende or hexagonal wurtzite structure. In this structure, each anion remains surrounded by four cations at the corners of a tetrahedron, and vice versa. This type of tetrahedral coordination generally speaks of  $sp^3$  covalent bonding nature, but these materials also show remarkable ionic nature that tends to increase the bandgap well above from what we expect from any covalent bonding. ZnO, even after being a II-VI semiconductor has an ionicity value which lies between that of the covalent and ionic semiconductors.

The crystal structures showed by ZnO are wurtzite (B4), zinc blende (B3), and rocksalt (or Rochelle salt)(B1) as schematically shown in Figure 1.1. B1, B3, and B4 denote the Strukturbericht designations for the three phases. Under ambient conditions, the thermodynamically stable phase of ZnO is that of wurtzite symmetry.

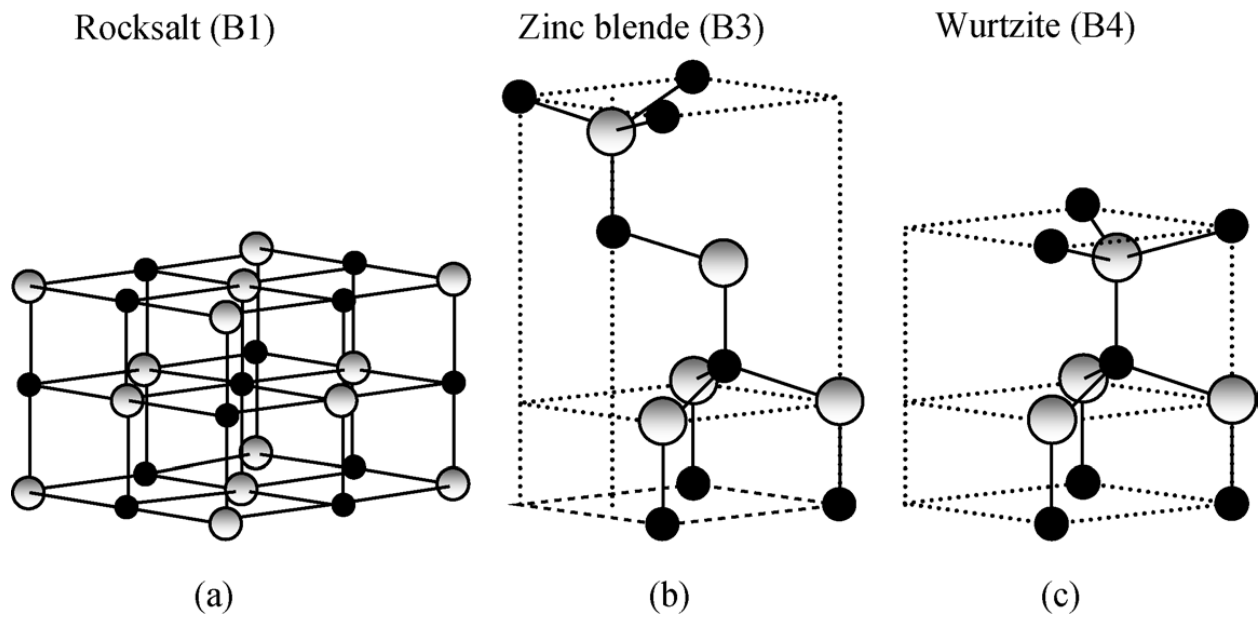


Figure 1

Stick-and-ball representation of ZnO crystal structures:  
 (a) Cubic rocksalt (B1), (b) cubic zinc blende (B3), and  
 (c) Hexagonal wurtzite (B4). Shaded gray and black spheres  
 denote Zn and O atoms, respectively.

### 3. SYNTHESIS OF MATERIALS

There are several methods of preparing thinfilms of ZnO which includes spin coating, dip coating etc. We use the spin coating method as this method is very easy compared to others and the precursor materials required for this method are easily available in the market. Besides, this method helps us get smooth films of ZnO at room temperature.

#### I. SYNTHESIS OF ZnO 1:

This was prepared using the precursor material Zinc Acetate Dihydrate and Ethanol as solvent.

3.9332g of Zinc acetate Dihydrate was dissolved in a mixture of 29.349ml of Ethanol(99.5% Hychem laboratory,  $\text{CH}_2\text{CH}_2\text{OH}$ ), 645 $\mu\text{l}$  of DI water and 5.543 $\mu\text{l}$  of HCL(conc.). This mixture was kept for overnight stirring at 40 $^\circ\text{C}$ . After overnight stirring, a clear transparent solution was obtained which was filtered using spin filters. This sol was stored and was used for developing thin film of ZnO over glass substrates using Spin coating method and consecutively heating the film at a temperature of 250 $^\circ\text{C}$  for 15 minutes.

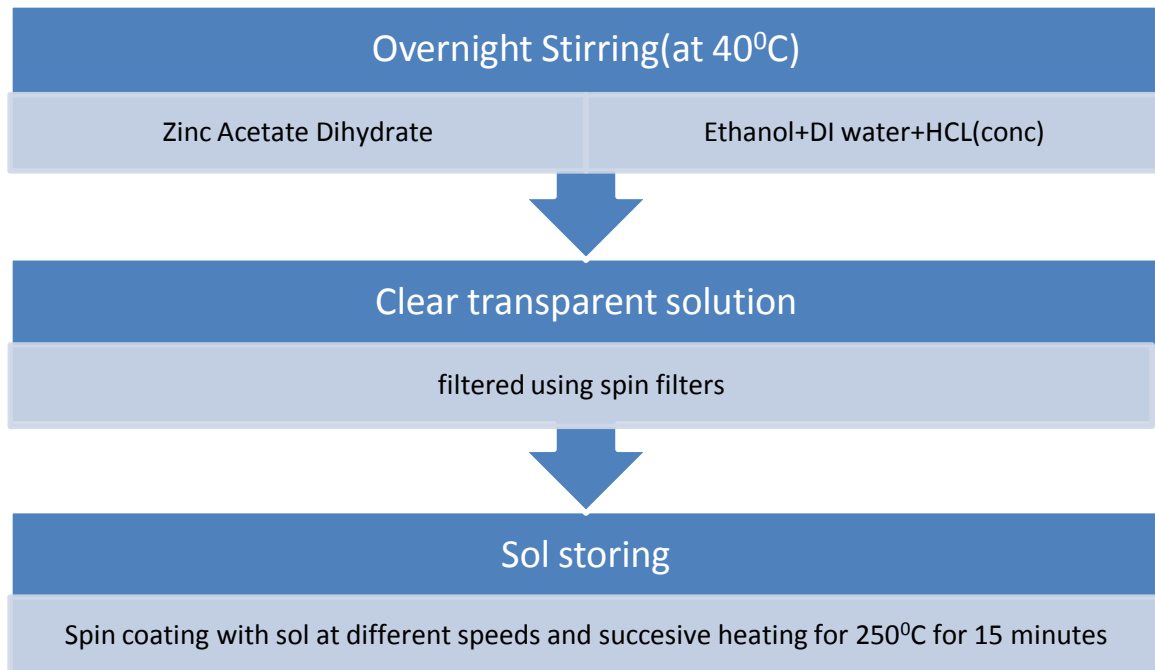


Figure 2

## II.SYNTHESIS of ZnO 2:

This was prepared using the precursor material Zinc Acetate Dihydrate and 2 methoxyethanol as solvent [10]

1g of Zinc acetate Dihydrate (Sigma Aldrich 99.999%) was dissolved in a mixture of 10ml of 2-methoxyethanol (Sigma Aldrich 99.5%) and 0.28g of ethanolamine (Sigma Aldrich 99.0%). This solution was kept for overnight stirring at room temperature in air. After overnight stirring, a clear transparent solution was obtained which was filtered using spin filters. This sol was stored and was used for developing thin film of ZnO over glass substrates using Spin coating method and consecutively heating the film at a temperature of 150<sup>0</sup>C for 1 hour.

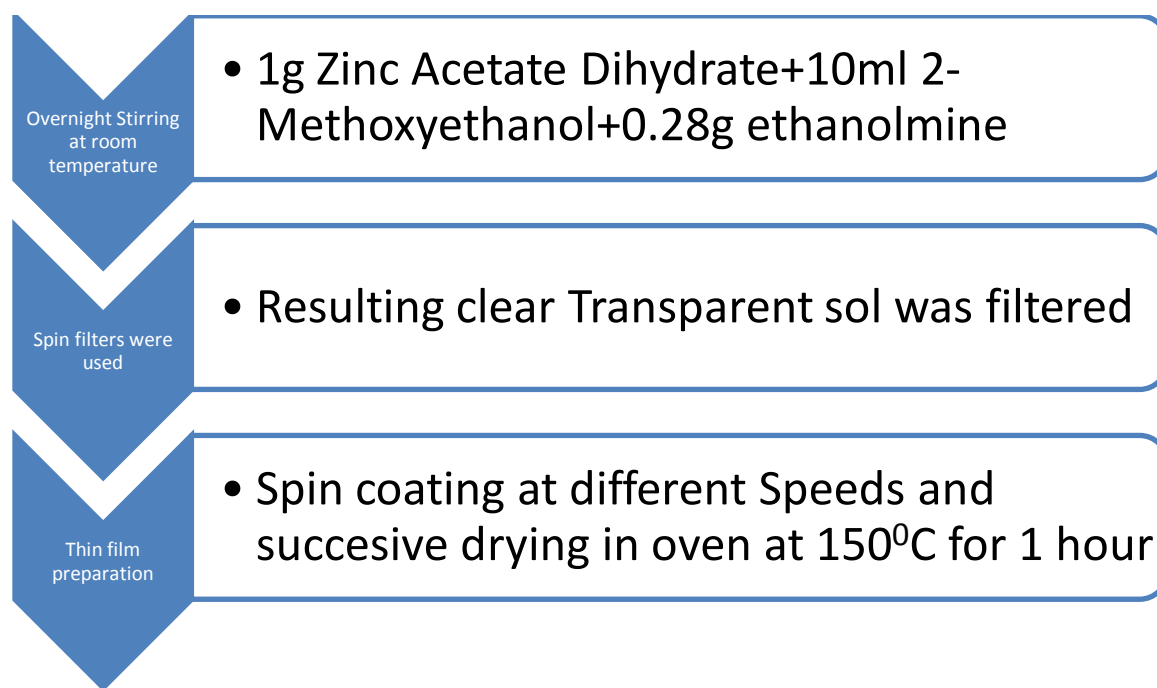
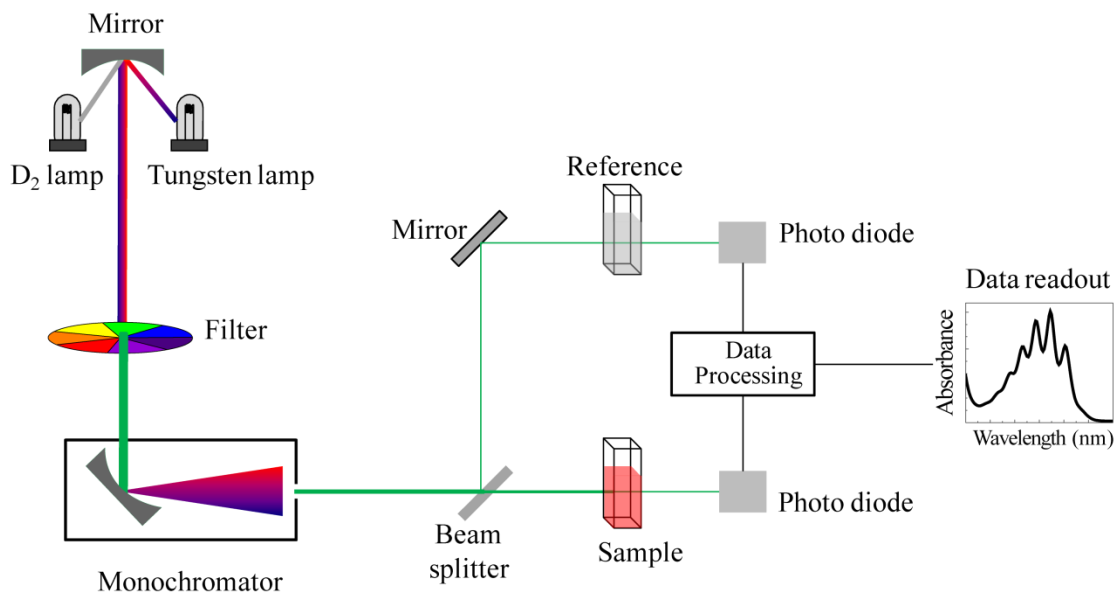


Figure 3

## CHARACTERISATION:

### I.UV Vis. SPECTROSCOPIC ANALYSIS:



**Figure 4**

UV Vis Absorption Spectroscopy is the type of absorption spectroscopy in which light of both UV and Visible wavelength (200-800nm) is absorbed by the molecule of the sample. Absorption of the radiations excites the electrons from the ground state to higher energy state. The energy of the radiation that is absorbed is equal to the energy difference between the ground state and higher energy states of the molecule.

UV Vis spectroscopy obeys the Beer-Lambert law, which states that: *when a beam of monochromatic light is passed through a solution of an absorbing substance, the rate of decrease of intensity of radiation with thickness of the absorbing solution is proportional to the incident radiation as well as the concentration of the solution.*

The expression of Beer-Lambert law is-

$$A = \log (I_0/I) = Ecd$$

Where, A = absorbance

I<sub>0</sub> = intensity of light incident upon sample cell

$I$  = intensity of light leaving sample cell

$c$  = molar concentration of solute

$d$  = thickness of sample cell (cm.)

$E$  = molar absorptivity

From the Beer-Lambert law, we get the idea that greater the number of molecules capable of absorbing light of a given wavelength, the greater the extent of light absorption. This is the basic principle of UV spectroscopy.

Light Source- 50 W Halogen lamps and Hydrogen-Deuterium lamps are used as a suitable light source as they cover the whole UV and Visible region.

Monochromator- Monochromators are generally composed of prisms and slits. The various wavelengths of the light source which are separated by the prism are then selected by the slits such the rotation of the prism results in a series of continuously increasing wavelength to pass through the slits. The beam selected by the slit is monochromatic and further divided into two beams with the help of another prism.

Sample and reference cells- One of the beams is passed through the sample and second beam is passed through the reference sample.

Detector- Two photocell serves the purpose of detector. One of the photocell receives the beam from sample and second detector receives the beam from the reference. The intensity of the radiation from the reference cell is stronger than the beam of sample cell which results in the generation of pulsating or alternating currents in the photocells.

Amplifier- The alternating current generated in the photocells is transferred to the amplifier. The current generated in the photocells is of very low intensity, so the main purpose of amplifier is to amplify the signals many times so that we can get clear and recordable signals.

Recording devices: Computer stores all the data generated and produces the absorption of our sample.



The following is the arrangement of the UV Vis Spectrophotometer used-

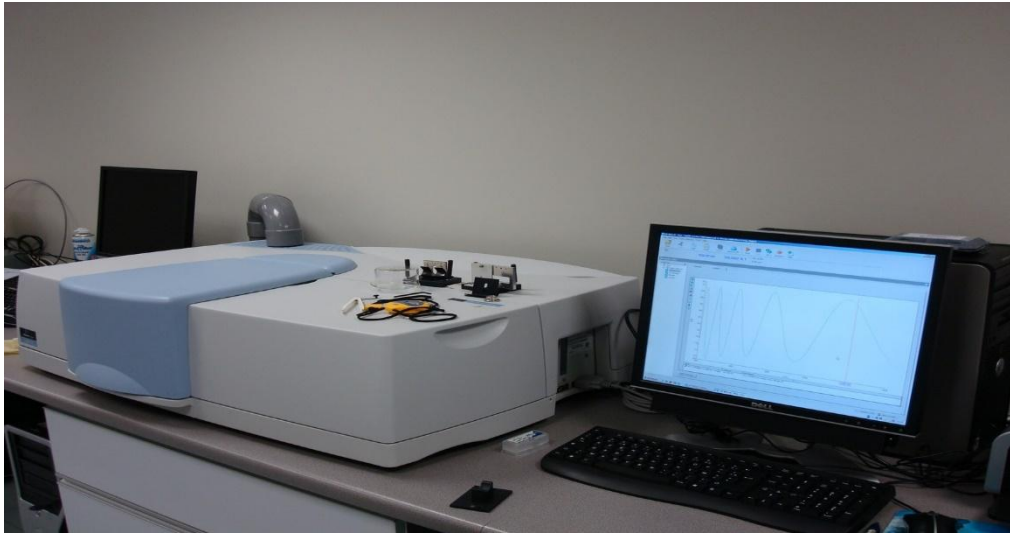


**Figure 5**

### **RESULTS AND DISCUSSION:**

For the sample ZnO 1, we the UV Vis Spectral analysis showed a plot as given below. Clearly we can see that the plot has peaks which correspond to the band gap of ZnO i.e. around 3.37eV.

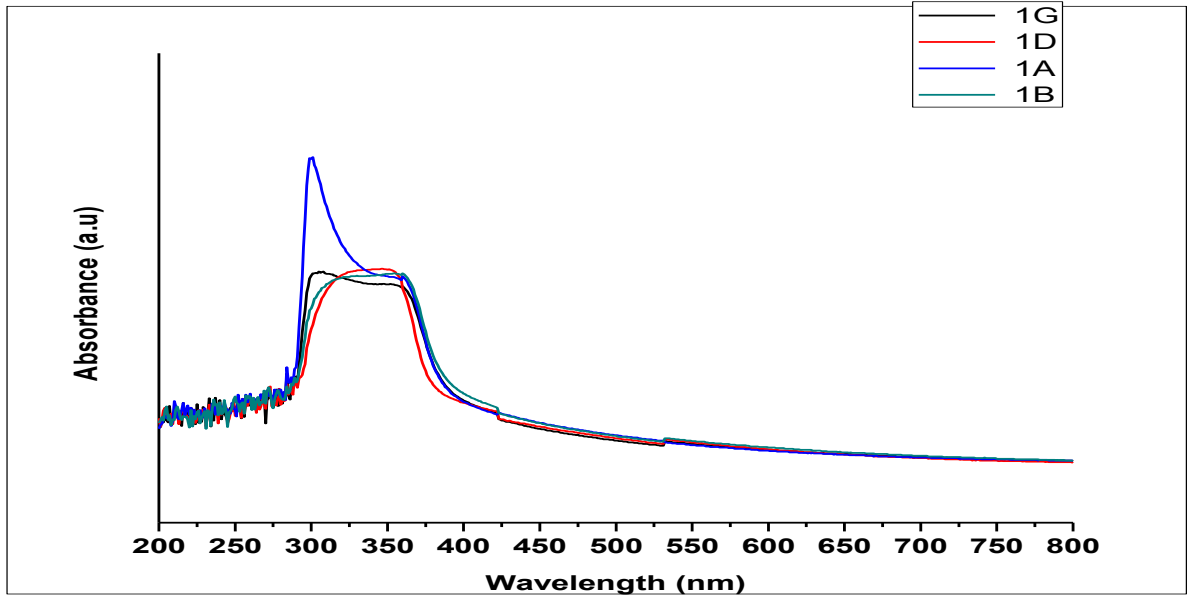


**Figure 6 UV Vis Absorption for ZnO 1 samples**

Sl no.	Sample No.	RPM	RPM duration(seconds)	Drying temp.( <sup>0</sup> C)	Drying Time(mins)
1	1A	1000	60	300	30
2	1B	1000	60	300	30
3	1D	1000	60	250	30
4	1G	1000	60	350	30

**Table 1**

The tauc plots of these graphs are provided below

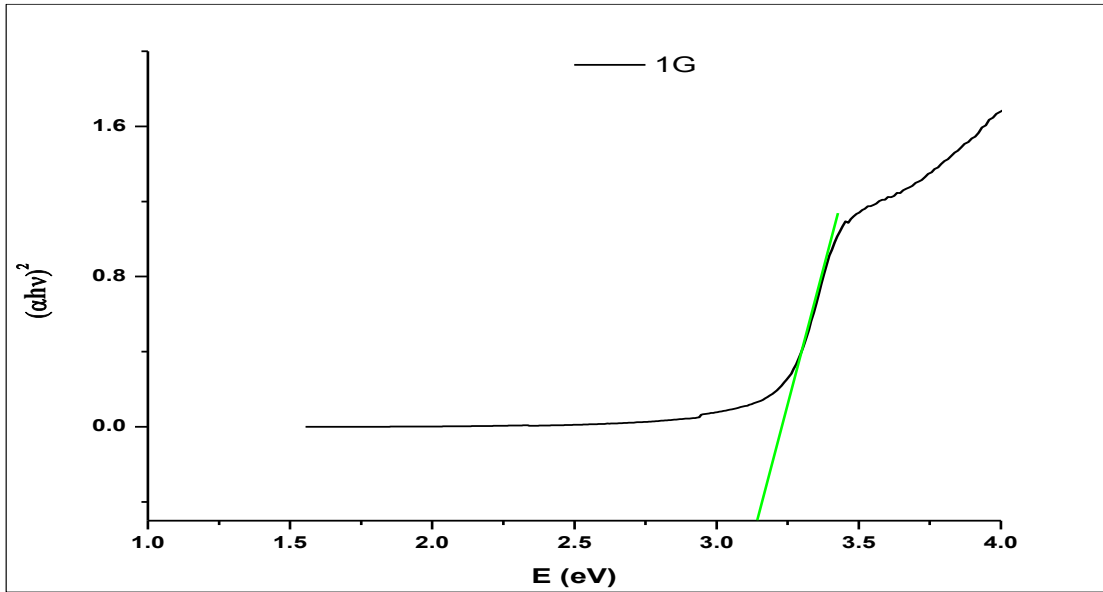


Figure 7 Tauc Plot of 1G

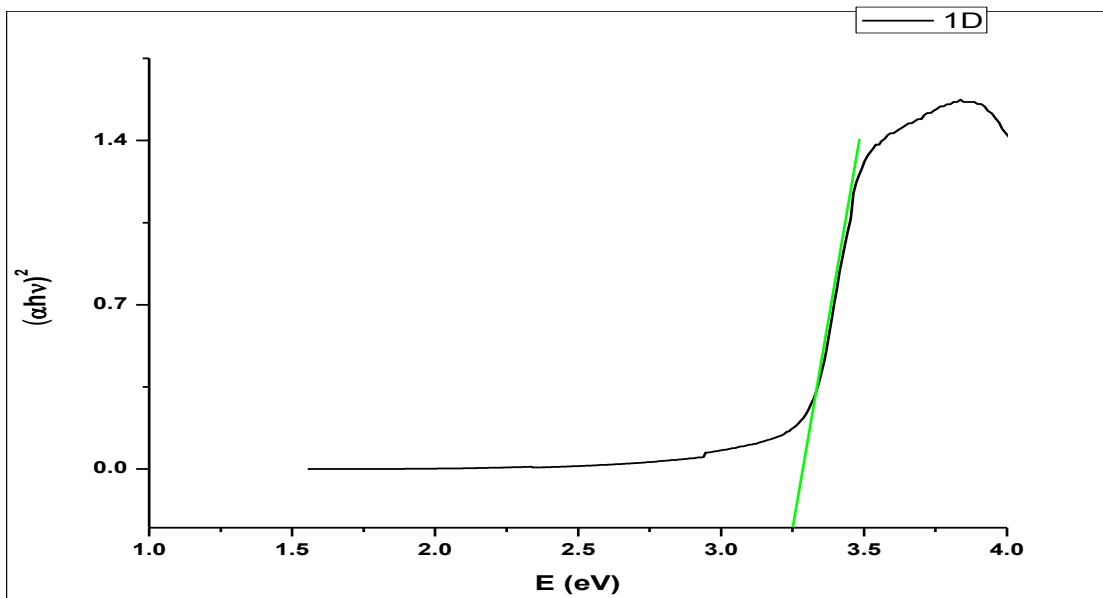


Figure 8 Tauc Plot of 1D

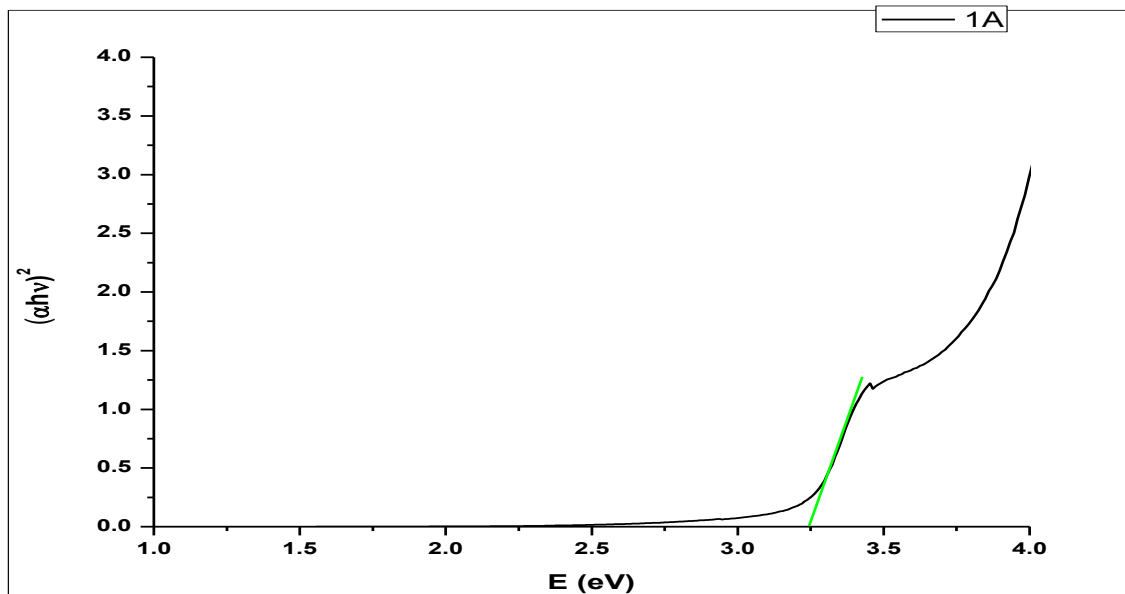


Figure 9 Tauc plot of 1A

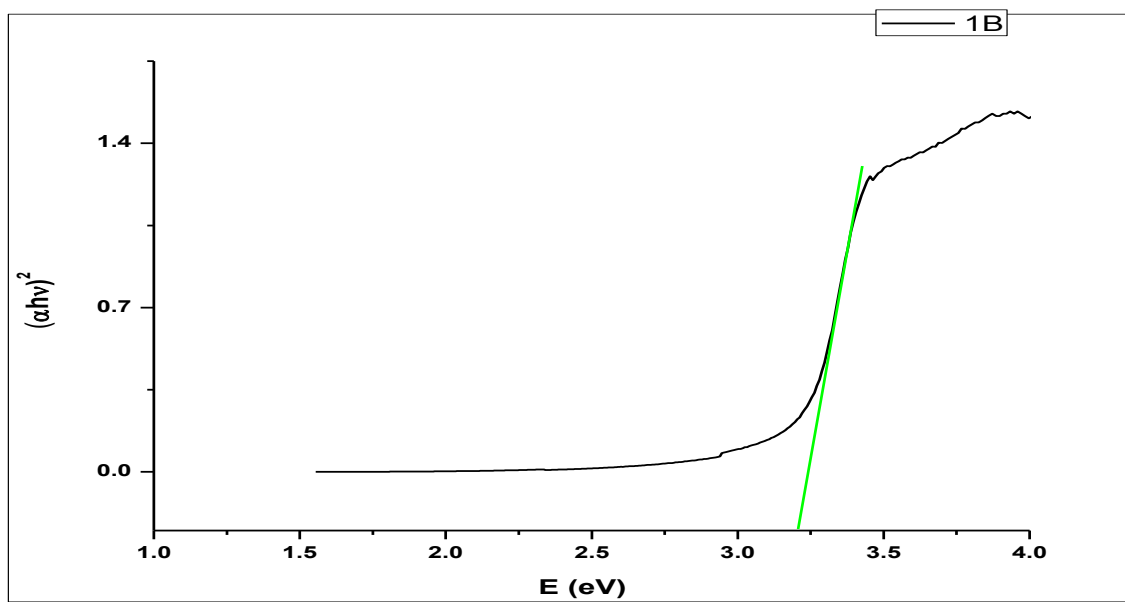


Figure 10 Tauc plot of 1B

Sl no.	Sample name	Band Gap(eV)
1	1G	3.14
2	1D	3.25
3	1A	3.25
4	1B	3.21

**Table 2 Band Gap energy calculated from Tauc Plot**

For ZnO 2, we obtain the following UV Vis plots:

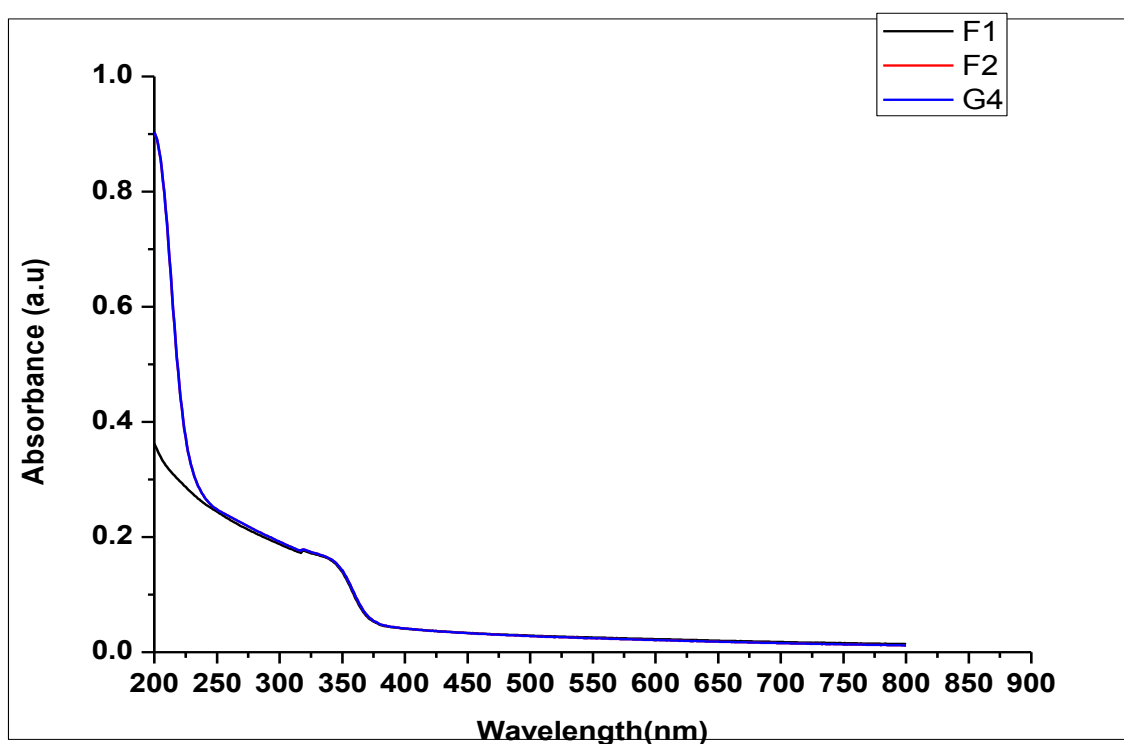


Figure 11 UV Vis plots for different samples of ZnO 2

Sl. No.	Sample no.	RPM	RPM duration(seconds)	Drying Temp( <sup>0</sup> C)	Drying time(minutes)
1	F1	1500	60	150	60
2	F2	1500	60	150	60
3	G4	1500	60	150	60

**Table 3**

The Tauc plots for these samples which gave us the values of their band gaps are given below:

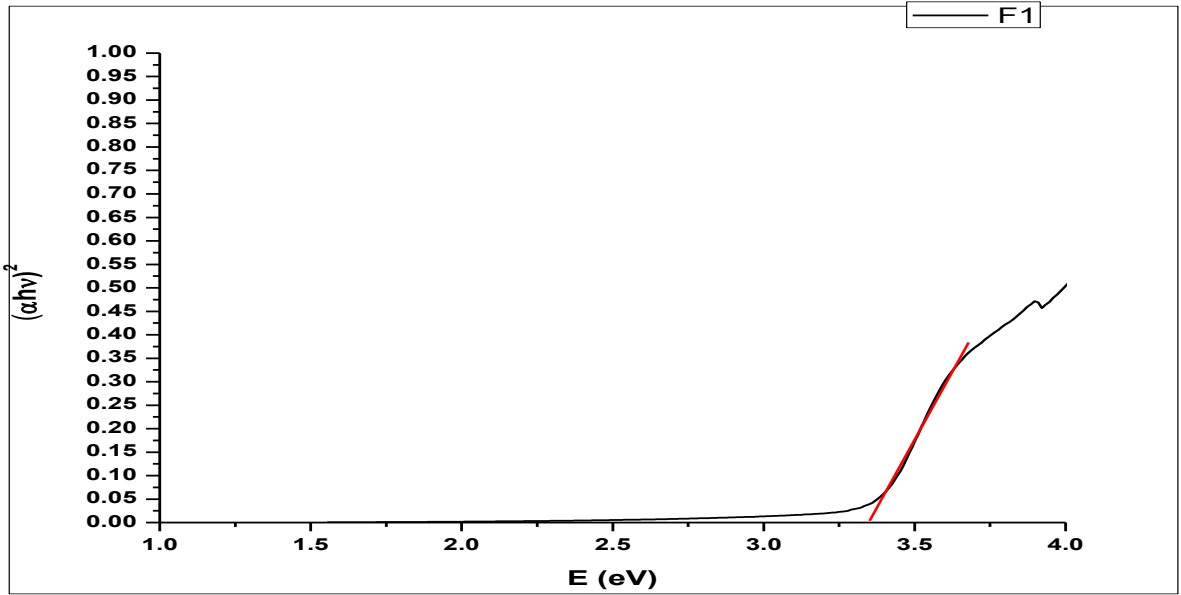


Figure 12 Tauc plot for Sample F1

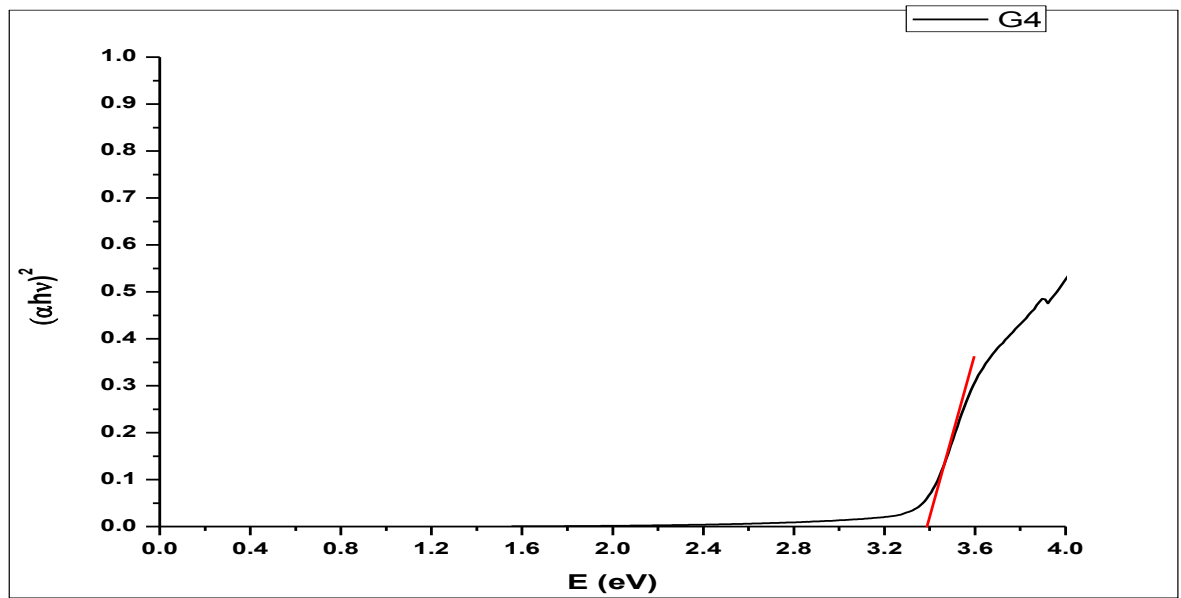


Figure 13 Tauc Plot for sample G4

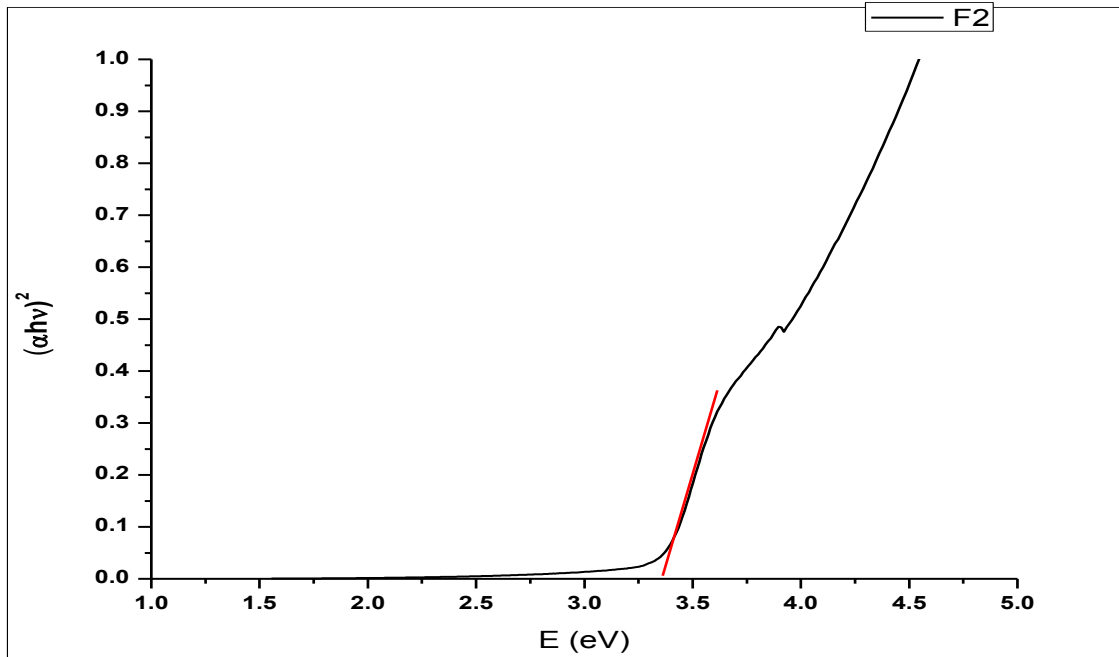


Figure 14 Tauc Plot for sample F2

Sl no.	Sample no.	Band Gap energy(eV)
1	F1	3.35
2	F2	3.35
3	G4	3.38

**Table 4 Band Gap energy calculation of the samples from respective Tauc Plot**

## II.XRD Measurement:

X-ray diffraction is an analytical method to identify and quantitatively determine various crystalline forms of compound present in samples. Diffraction occurs due to interaction of waves with the repeated periodic structure of the compound in the sample. Needless to say the wavelength of the incoming waves should be of the order of the periodic structure of the sample. Since we have X-rays whose wavelengths are of the order of a few angstroms, which is same as typical inter-atomic distances in crystalline solids. Thus X rays can be used to determine the structure of materials which are crystalline. At certain conditions, X-rays scattered from a crystalline solid can interfere constructively, producing a diffracted beam. In 1912, W. L. Bragg first recognized a relationship among several factors and gave the following relation:

$$n\lambda=2d\sin\theta ,$$

$\lambda$ - Wavelength of X-ray

d-interplanar spacing,

$\theta$ -diffraction angle

n-0,1,2,3...

The low diffraction intensity from a thin top layer in a  $\theta$ - $2\theta$  scan is because of the fact that path length of the X-rays in the thin film is very short. Therefore, most of the radiation interacts with the underlying substrate. In addition to lower peak intensity in  $\theta$ - $2\theta$  scans, the thin-film reflections may also get superimposed and may make it difficult to distinguish from substrate reflections. This in turn complicates the evaluation of the XRD data. In order to improve the situation for thin films, low-angle XRD techniques such as grazing incidence X-ray diffraction (GIXRD) have been developed.

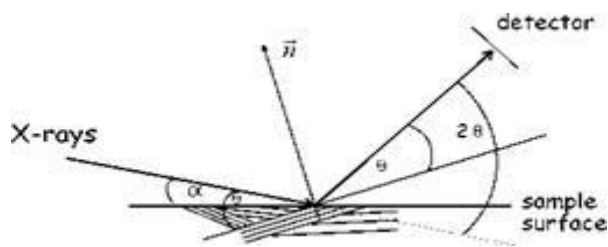


**Figure 15 Principle geometry of GIXRD experiment:  $\alpha$ – incident angle,  $\theta$  – Bragg angle, n – normal of the lattice plane which fulfills the Bragg equation**



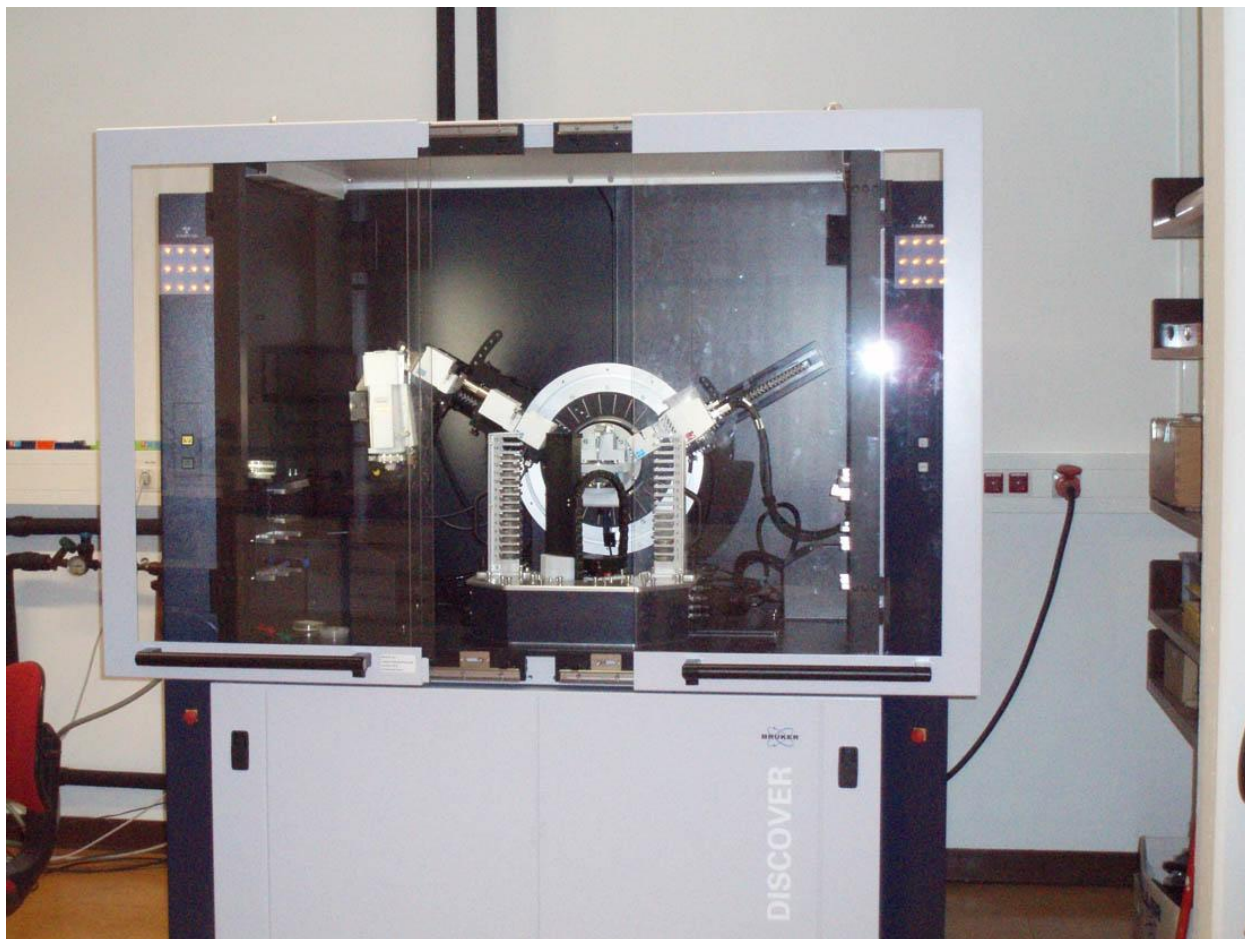


**Figure 16 Instrument for GIXRD analysis (BRUKER D8 DISCOVER)**

## **RESULTS AND DISCUSSION:**

The GIXRD pattern for ZnO 1 shows the following pattern:

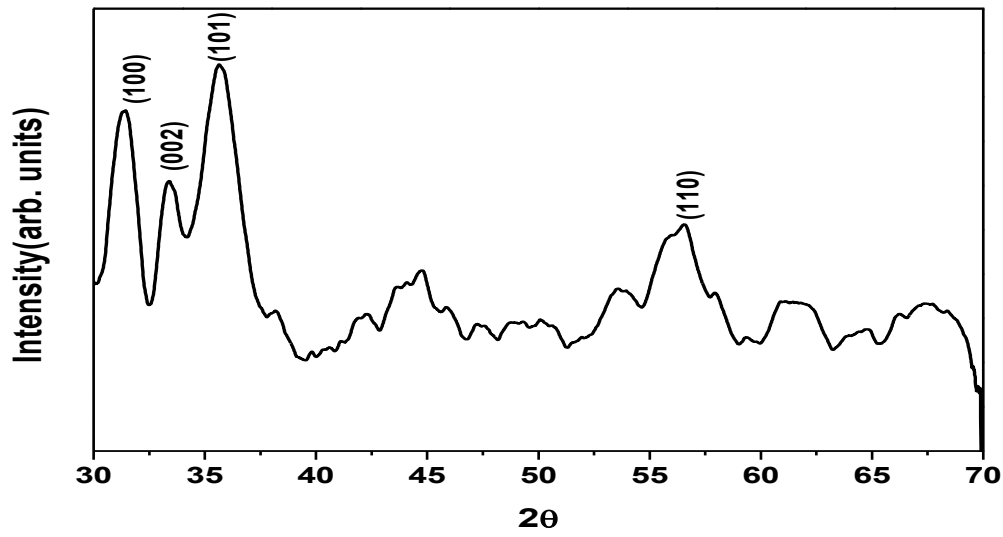


Figure 17 XRD of ZnO 1

The JCPDS value of the Hexagonal ZnO is given as:

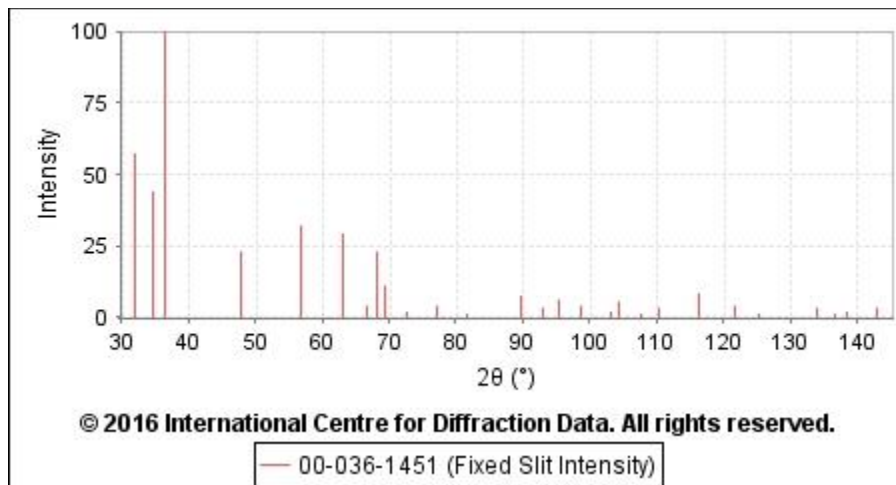


Figure 18

As we can see that along with the observation of certain peaks which resemble the hexagonal structure of ZnO, we also obtain some other peaks which indicate the presence of impurities in the sample.

The GIXRD pattern for ZnO 2 is given below:

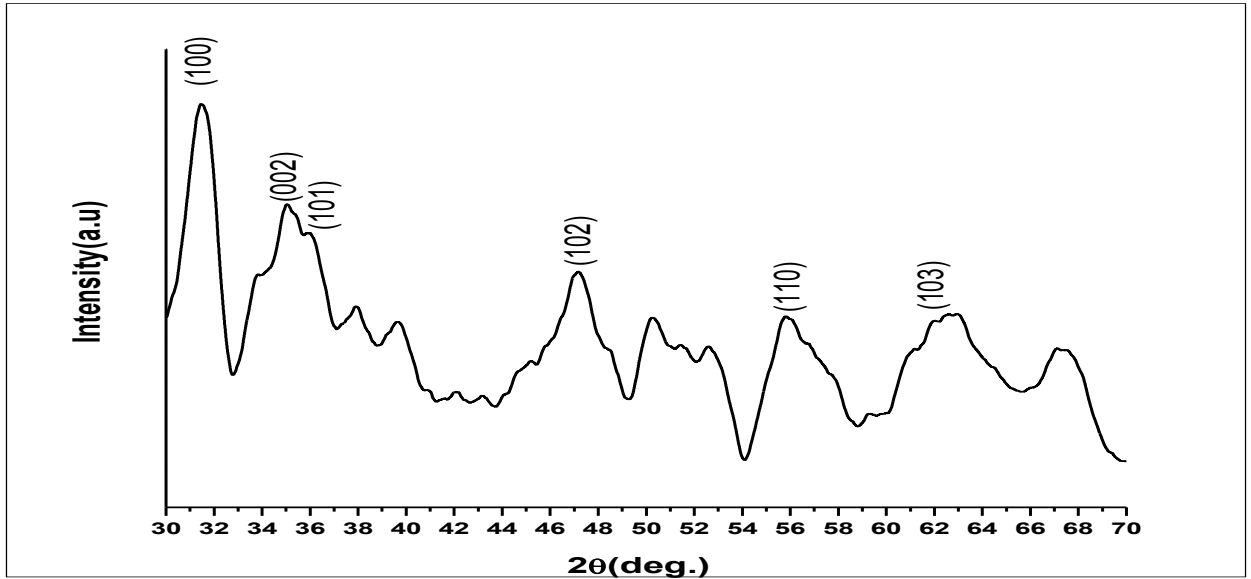


Figure 19 XRD of ZnO 2

Here finally we obtain some peaks most of which indicate the hexagonal structure of ZnO. Apart from these, there are certain other peak which as usual defines the existence of certain other impurities in the sample.

### III. Optical Profilometer Measurement:



**Figure 20 Arrangement of Optical Profilometer**

Test surfaces and features are clearly visible only when they are within the focal depth. This system scans a sample over a user specified vertical (or Z) range. At each Z position, it records the XY location and the precise Z height of the pixels using the Optics Module. This information is used to create a true color 3D image and a 2D composite image. The resulting image has an extended depth of focus so the entire surface is seen clearly.

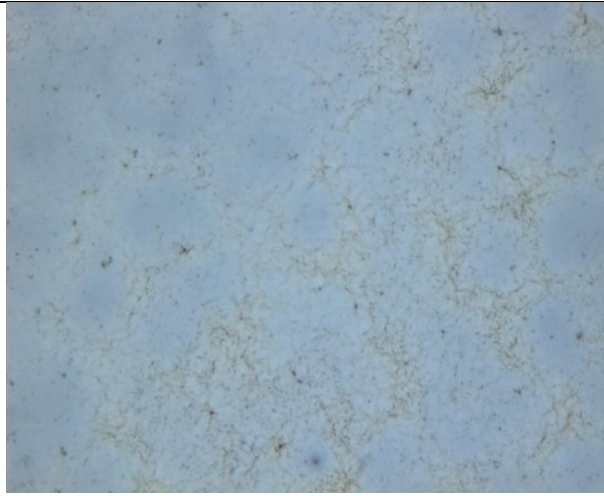


Figure 21-F2 2D image(Field of view-  
189 $\mu$ m $\times$ 142 $\mu$ m)

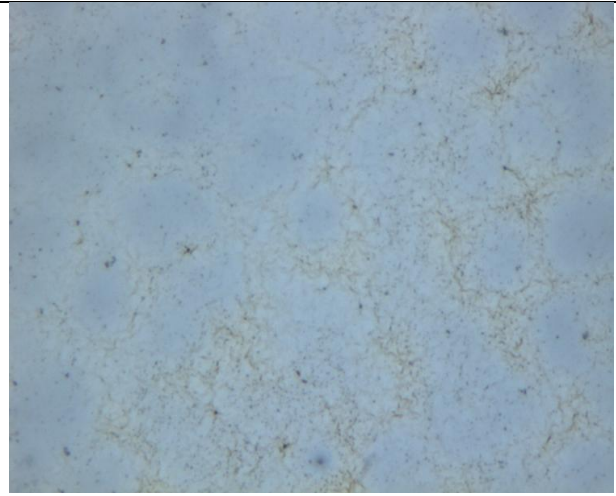


Figure 22- G4 2D image(Field of View-  
189 $\mu$ m $\times$ 142 $\mu$ m)



Figure 23- S1 Roughness(FOV-94 $\mu$ m $\times$ 71 $\mu$ m)

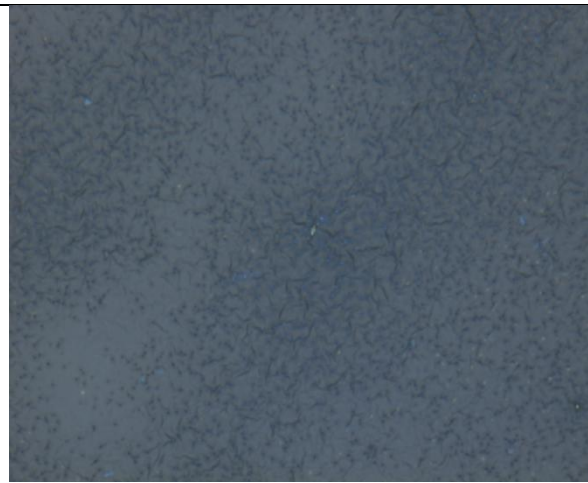


Figure 24- N1 Roughness(FOV-94 $\mu$ m $\times$ 71 $\mu$ m)

Looking at the images, we can notice that the light and dark bands are not same all over the image. This is because the lower portion of the interferogram is going out of focus which means less interference. By carefully calculating the area of greatest contrast, optical profilometers determine the point that has best focus. Since the thin films are not uniform, hence we observe areas with various contrasts.

Sl no.	Sample name	RPM	Stage	Time(seconds)	Roughness( $\mu\text{m}$ )	Standard deviation	Variance
1	F2	1500	Single	60	0.0606	0.0058	9.60%
2	G4	1500	Single	60	0.0638	0.0103	16.2%
3	N1	1500	Four	60	0.0216	0.951nm	4.40%
4	S1	1500	Four	60	0.0159	0	0%

**Table 5**

Thus from our observation, we can infer that the roughness of the samples for single stage coat is around 60.6nm-63.8nm while that for four stage coating, it varies from 15.9-21.6nm.

The thicknesses of the samples were also measured using Zeta 3D profilometer. Since the film deposited on the substrate was not smooth, it contained air bubbles in it. This air bubbles made the substrates visible from outside. Hence the area at the junction of the air bubble and the film was marked and the profilometer was zoomed over it. The contrasting images that were obtained provided us the thickness of the film.

Sl no.	Sample name	RPM	Stage	Thickness( $\mu\text{m}$ )	Standard Deviation	Variance
1	N1	1500	Four	0.1065	0.0121	11.3%
2	S1	1500	Four	0.1012	0.0049	4.85%

**Table 6**

Hence from our observation, we can infer that the thickness of four stage coating of our sample varies from 101.2nm-106.5nm.



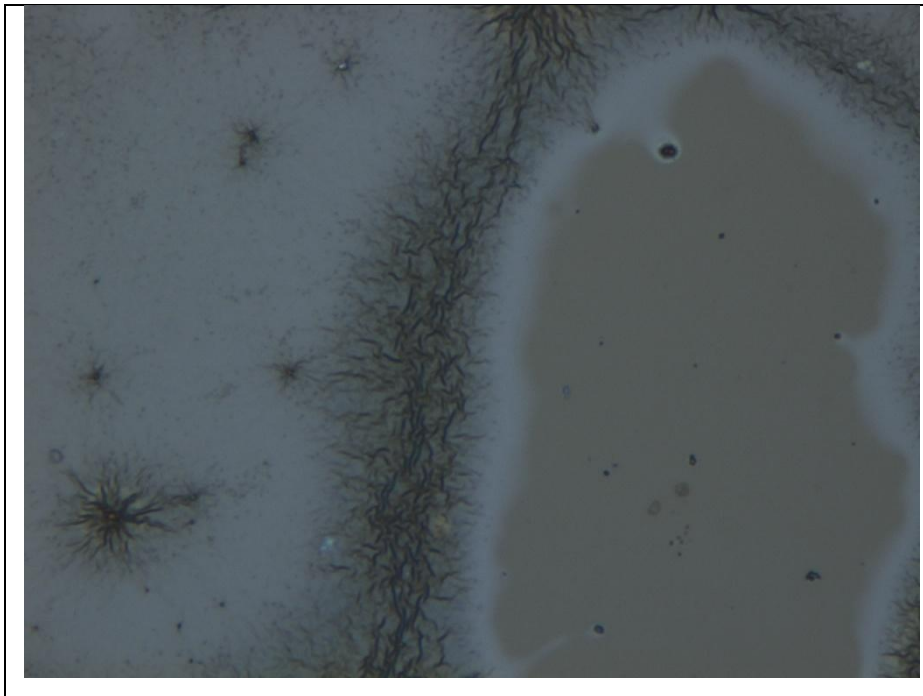


Figure 25S1 film thickness (field of view: -189 $\mu$ m x 142 $\mu$ m)

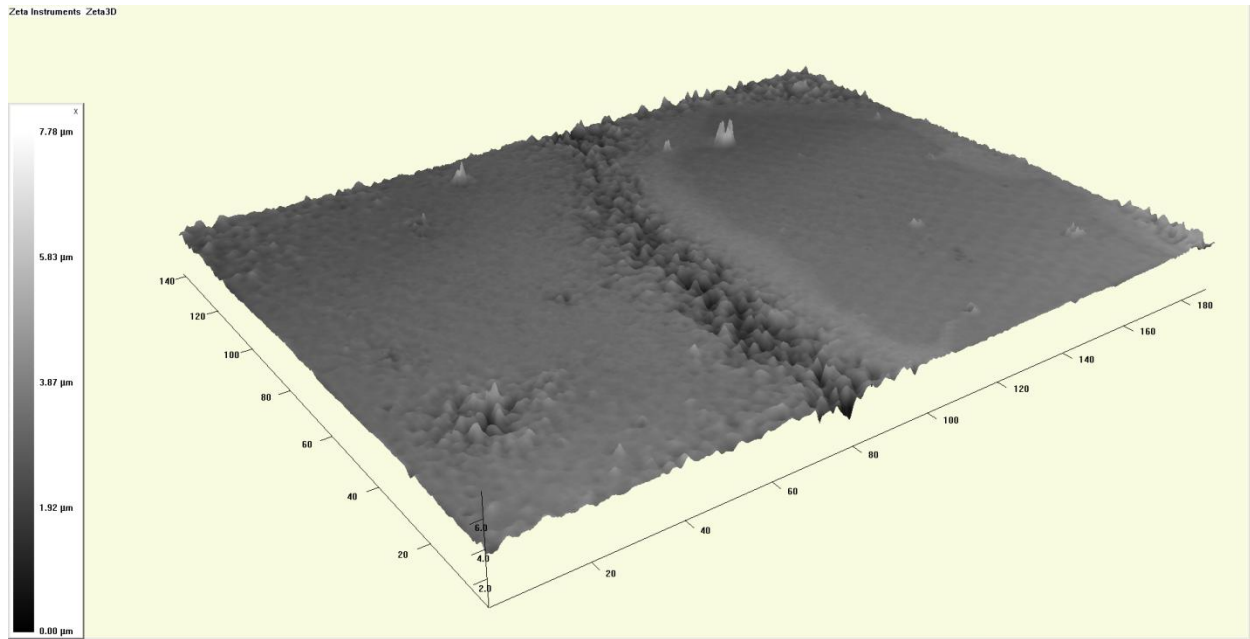
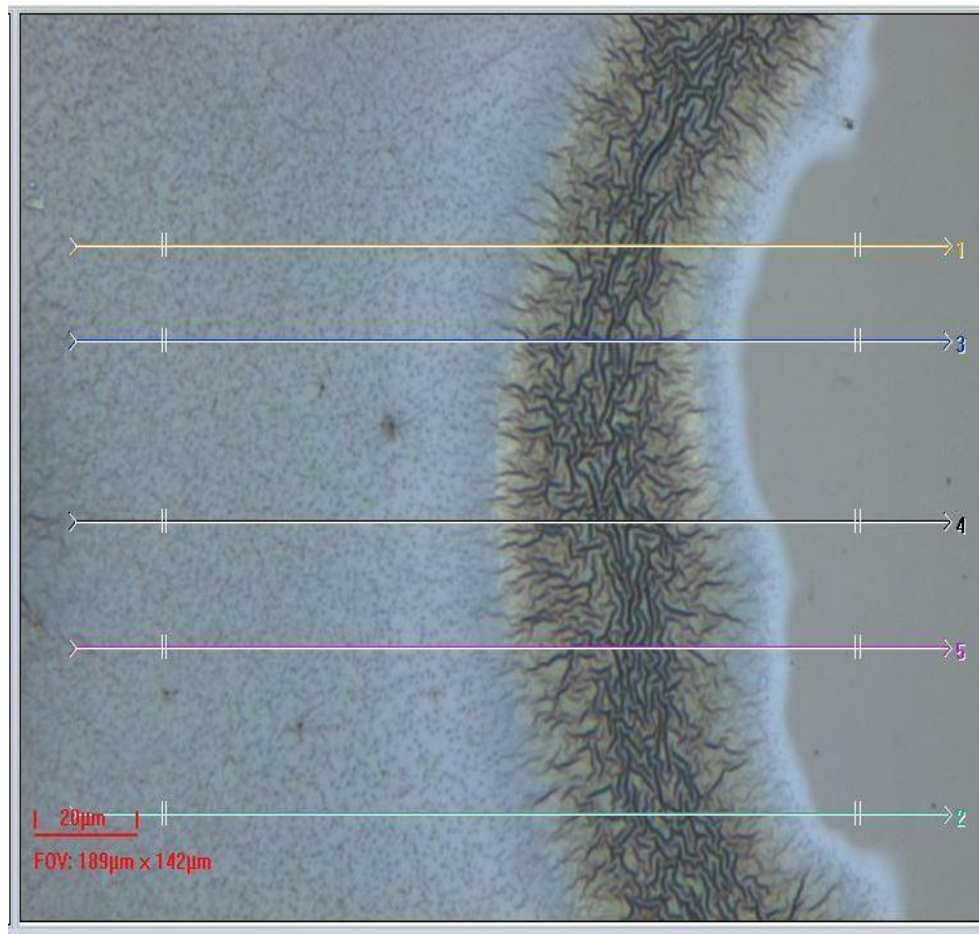
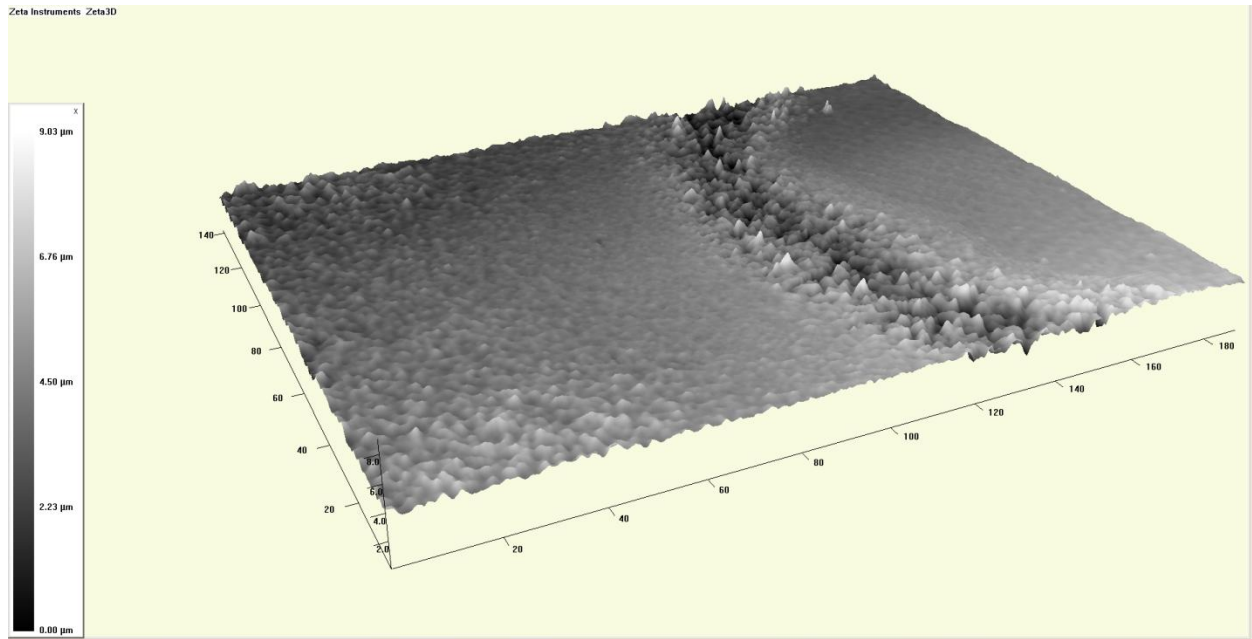


Figure 26 S1 Film Thickness 3D (field of view: -189 $\mu$ m x 142 $\mu$ m)





## **5.Dye G1 and Dye ZnO interface:**

### **5.1 Dye: G1**

In DSSC, the dye molecule is responsible for optical feature of the system – it facilitates absorption of light in solar spectrum. A good overlap of energy levels between the lowest unoccupied molecular orbital (LUMO) of the dye and conduction band of the semiconductor, as well as mixing of these energy levels, are important factors to initiate a fast electron transfer into the conduction band of the semiconductor. Electron transfer from the excited dye to the semiconductor should process as fast as possible to decrease the recombination rate with the corresponding hole.

Anthrance derivative of organic dye G1 which is provided by Dr. Giribabu from IICT. The optical properties of organic dye G1 is given by the highest occupied molecular orbit lies at energy 4.95 eV and lowest unoccupied molecular orbit lies at energy of 2.74 eV. And the band gap for the Dye: G1 molecule is 2.21 eV. Its structure is shown in the figure below. The carboxyl group (COOH) is the anchor group, with which the molecule binds to a semiconductor surface.

Figure 29 **Structure of the G1 molecule**

## 5.2 Preparation of ZnO and Dye G1 interface:

G1 and ZnO interface was prepared by Chemical bath deposition process. The ZnO thin films grown over FTO substrates were allowed to soak in a container containing the G1 dye for around 17 hours.

Bonding Configuration:

G1 has carboxyl group that would be bind with ZnO either by molecular or dissociative adsorption. Several binding studies agrees that the most probable binding configuration is through one COOH group where the OH group is replaced by ZnO molecule as shown in figure.

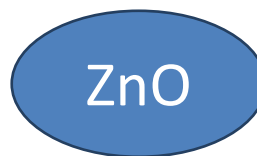


**Figure 30** Structure of the G1 and ZnO interface

The dye molecule is responsible for absorption of light. ZnO has an optical band gap of 3.4 eV and can only absorb light with wavelengths less than 365.6 nm. Since the optical band gap of G1 on ZnO is 2.4 eV, the G1 dye molecule is able to absorb light in the visible and near infrared spectrum and covers therefore the emission peak of the solar spectrum (518 nm, 2.4 eV).

As the dye molecule absorbs a photon with an appropriate energy, an electron is excited from the highest occupied molecular orbital (HOMO) to the lowest unoccupied molecular orbital (LUMO).

Since both of these possess a certain energy width, a continuous spectrum of photon energy can be absorbed.

The absorption of a photon leads to the creation of an electron-hole pair, which must be separated in order to produce current. The electron is transferred into the semiconductor and the hole in the dye molecule is filled by donation of an electron from a negative ion of the electrolyte solution. The alignment of the involved energy levels here is of great importance. The LUMO level must be located above the conduction band minimum, for electron transfer into the semiconductor to occur. The hybridization of molecular levels (in particular the LUMO) with the substrate can play an important role in electronic transfer. A LUMO that is highly delocalized over the substrate will allow a fast electron transfer from the dye to the substrate. The ionization potential of the electrolyte-redox pair has been located above the HOMO level of the dye molecule, in order to refill the hole in the dye molecule by an electron from the electrolyte. The process of electron-hole separation occurs for ZnO in a typical time scale of 100 ps. Efficient electron transfer to the conduction band avoids recombination of the electron with the hole, as well as energy and voltage loss by relaxation to the bottom of the semiconductor conduction band.

Once an electron leaves the dye molecule, it is not trapped on the surface and enters the bulk of ZnO. While the electron diffuses through the bulk to the electrode, it relaxes to the bottom of the conduction band, which is thought to occur by vibration coupling. If the electron returns or remains trapped at the surface, it combines with the positive charge residing on the electrolyte mediator.

#### Limitations in The Arrangement of Energy Levels:

As mentioned, the peak of emission of sunlight is at a wavelength of 518 nm (2.4 eV). The sun possesses a continuous spectrum of light from infrared to ultraviolet. The power output of an electrical device is defined in general as the product of current and voltage. The closed-circuit current and open-circuit voltage both are dependent on the energy alignment of the HOMO and LUMO levels of the dye.

The closed circuit current of solar cell is dependent on the intensity of the incoming light and the absorption spectrum of wavelengths is limited in a DSSC in higher wavelengths. In order to increase the current of a DSSC, the dye molecule should adsorb light with wavelengths up to 900 nm, which can be managed by a decreased HOMO – LUMO gap. The HOMO – LUMO gap cannot be decreased arbitrarily since this energy gap is directly related to open circuit voltage of DSSC.

### 5.3 Experimental Setup:

#### 5.3.1 Photoluminescence Fluorimeter system:

The spectrofluorimeter contains a 450 W xenon CW lamp as a steady state excitation source and a pulsed xenon lamp for phosphorimetry. The light path is directed to a double – grating monochromator where the slit size and wavelength are calibrated all the times. The sample compartment is bifurcated to accommodate two monochromator/detector sets: one consists of a single grating monochromator attached to a fully automated iHR spectrometer with dual detection mode (250-1050 nm) and a single monochromator attached to a thermoelectrically cooled InGaAs NIR PMT module (950- 1400 nm). All detectors are operated in the single photon counting mode; the signals from the detector are then amplified and sent to a data acquisition system and a computer.



**Figure 31 Image of experimental setup for emission spectrum**

The shape and intensity of fluorescence spectrum is highly dependent on the nature of the sample, its concentration, and solvent choice. Given that small particles within the solution induce light scattering, the scattered photon may find their way to detector introducing measurement errors. The fluorescence intensity is linearly dependent on the sample concentration over limited range optical densities. The threshold concentration above which deviation from the linear behavior is observed depends on the chromophore. Finally, it is strongly recommended once an excitation wavelength has been chosen, a plot of optical density versus fluorescence intensity is generated in order to determine if the measurement is done in linear regime and that there is no reabsorption.

## **5.4 Result and Discussion**

In general dyes dissolve in monomers, dimers, trimers, etc. At low concentrations monomers dominate. With increasing concentration dimers and higher aggregates may gain importance. Each component (monomer, dimer, etc.) may have a different absorption behavior. At high concentration the constituting components (monomers, dimers, trimers, etc.) of the solution come near together (statistical random walk distribution of constituents) and if two neighboring components are within an interaction volume, the mutual solute-solute interaction changes the absorption behavior.

### **5.4.1 Absorption Spectrum:**

The absorption spectra of ZnO, G1 dye and dye G1 + ZnO are recorded in the wavelength ranging from 300 – 800 nm. The absorption spectra of all the three are shown in figure. The G1 dye shows a broad absorption peak in visible region wavelength at 460 nm and in near UV region at 345 nm and it shows low absorption at wavelength 498 nm. The absorbance of Dye + ZnO interface increases and as shown in the figure, the peak near UV region at 345 nm is red shifted and absorption is more than the dye solution. Even the absorption in visible region at wavelength 460 nm increases. The figure shows that the absorbance of dye increases as ZnO is treated with it.

The UV Vis absorption behavior of the ZnO+G1 dye is shown in the plot below:

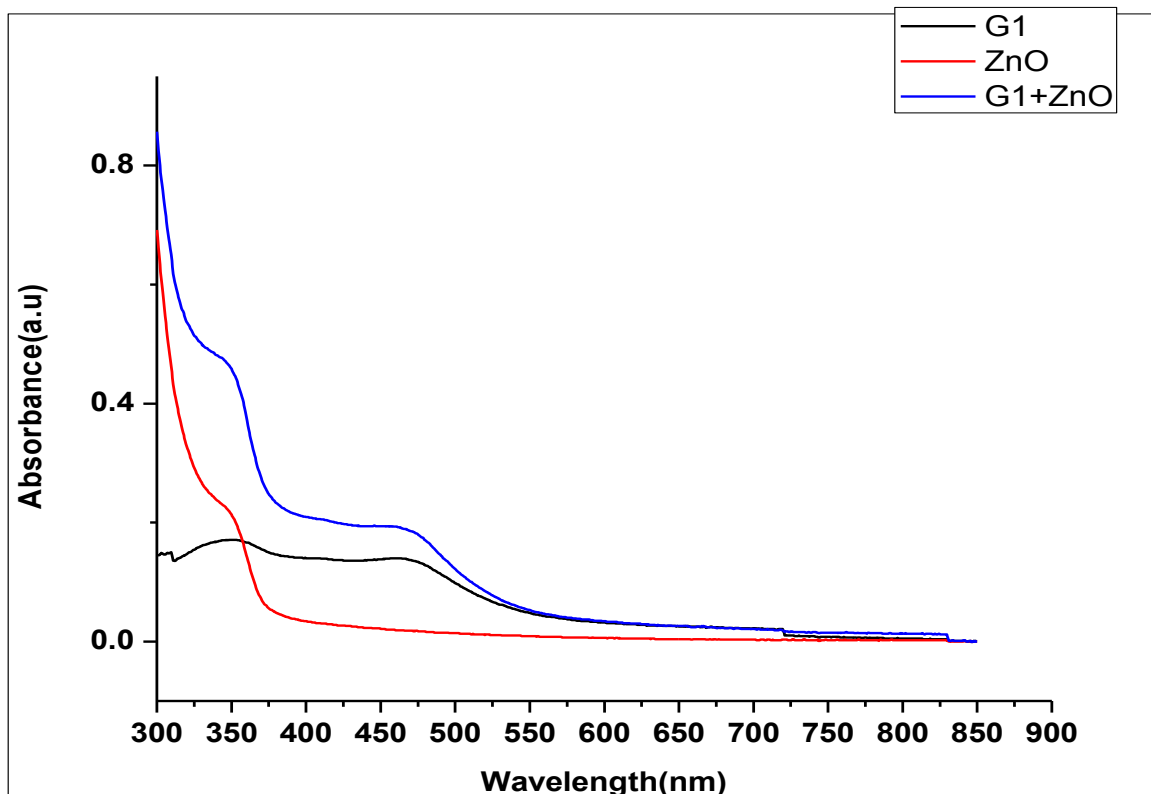


**Figure 32 The UV Vis absorption behavior of the ZnO+G1 dye**

Clearly we can see that the absorption of the dye G1 is enhanced by the presence of the ZnO. Thus the G1+ZnO interface can act as a better compound to absorb most of the emission of the sunlight as the band gap energy at the interface corresponds to 518nm of wavelength which is equivalent to 2.4eV.

#### 5.4.2 Photoluminescence Spectra:

##### **Excitation at 345nm:**

The photoluminescence spectra of Dye G1 and Dye G1 + ZnO are shown in figure, obtained at an excitation wavelength of 345 nm. It shows that the peak will be at 664nm which is the characteristic peak of the Dye G1 molecule. When dye G1 + ZnO emission spectrum was taken, the peak at 664 nm will reduce from its maximum value as shown in figure. It is mainly due to the electron transfer takes place from G1 to ZnO molecule.

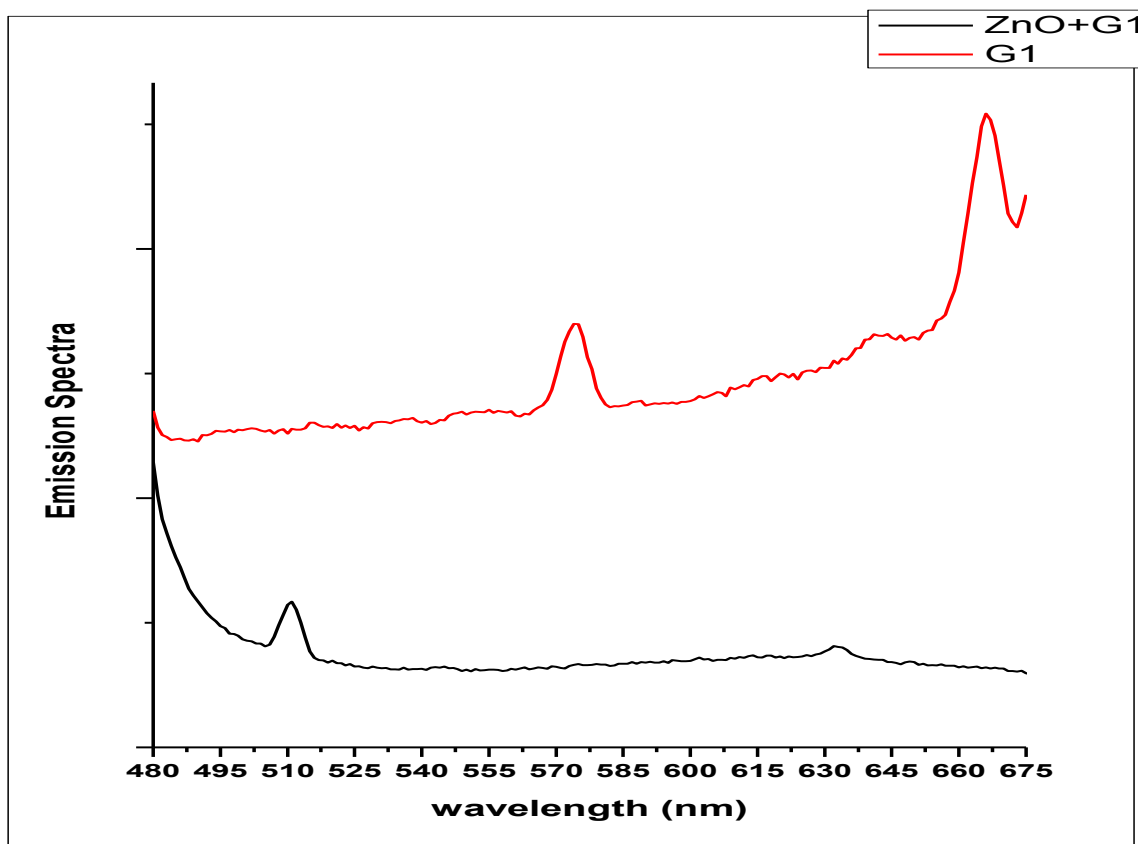


**Figure 34: Excitation at 345nm**

**Excitation at 460nm:**

The photoluminescence spectra of Dye G1 and Dye G1 + ZnO is shown in figure, obtained at an excitation wavelength of 460 nm. The peak is supposed to be at 664nm which is the characteristic peak of the Dye G1 molecule but we obtained a peak at 630nm. When dye G1 +ZnO emission spectrum was taken, the peak at 630 nm reduced from its maximum value as shown in figure. It is mainly due to the electron transfer takes place from G1 to ZnO molecule.



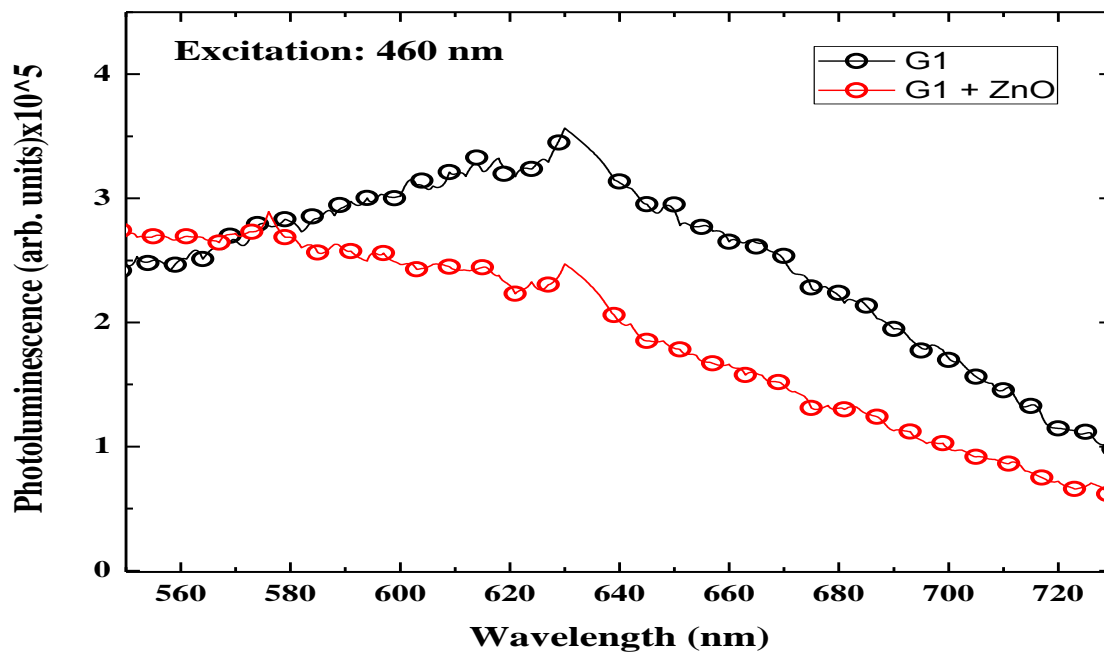


Figure 35: Excitation at 460nm

## 6.0-VARIOUS PARAMETERS IN A SOLAR CELL:

a)  $V_{OC}$ -The open-circuit voltage,  $V_{OC}$ , is the maximum voltage available from a solar cell, and this occurs at zero current. The open-circuit voltage is the amount of forward bias voltage on the solar cell due to the bias of the solar cell junction with the light-generated current.

b) **EFFICIENCY:** Efficiency is defined as the ratio of energy output from the solar cell and input energy from the sun. The efficiency of a solar cell is found out as the fraction of incident power which is converted to electricity and is defined as:

$$P_{max} = V_{OC} I_{SC} FF$$

$$\eta = (V_{OC} I_{SC} FF) / P_{IN}$$

where  $V_{oc}$  = open-circuit voltage;

where  $I_{sc}$  = short-circuit current;

where  $FF$  = fill factor

where  $\eta$  = efficiency.

c)  $I_{SC}$ : The short-circuit current is the current through the solar cell when the voltage across the solar cell is zero (i.e., when the solar cell is short circuited). The short-circuit current is the maximum current which can be drawn from the solar cell.

d) **FILLFACTOR (FF):** The short-circuit current and the open-circuit voltages are the maximum current and voltage respectively from a solar cell. However, at both of these points, the power from the solar cell is zero. The "fill factor" determines the maximum power from a solar cell. The FF is defined as the ratio of the maximum power from the solar cell to the product of  $V_{oc}$  and  $I_{sc}$ . In terms of graph, the FF is a measure of the area of the largest rectangle which may fit in the  $I$  vs.  $V$  curve.

## 6.1. Data from Solar Cell tester:

3 solar cells were prepared with different configurations using ZnO thin films as an interface. The Cell Tester model then tested the cell for its  $I$  vs.  $V$  plots which is described by the data mentioned below.



**Figure 36 Testing in progress in a solar tester**

### **6.1.1.-Preparing Solar Cells:**

#### **A) Preparing thin films of ZnO:**

Substrate used: FTO (Fluorinated Tin oxide)

Firstly the resistance was measured on the conducting side so as to ensure that we are not preparing the film on the wrong side. Next a substrate of an area 2.5X2.5 cm was cut out from it. After that an area of 5mmx5mm was marked on the conducting side and then films of ZnO 2 were coated using a spin coater. The following specifications were used for preparing these 3 samples-

Sl no.	Sample name	RPM	Stage	RPM duration(seconds)	Drying temp.( <sup>0</sup> C)	Drying duration (mins.)
1	2	1000	3	60	150	60
2	3	1000	3	60	150	60
3	4	1000	10	60	150	60

**Table 7**

After preparing these samples, the excess area was cleaned of the ZnO film using the Dichloromethane (This has also been used to solvent for the G1 dye).

Meanwhile we prepared the electrolyte which is needed for the solar cell operation.

**B) Preparing Electrolyte:**

The electrolyte is prepared using the following concentrations:

0.05M I<sub>2</sub>

0.1M LiI

0.6M Imidazolium Cyanide

0.5M Tert butyl pyridine

Acetonitrile as solvent

**CALCULATIONS:**

Wt. of I<sub>2</sub> =  $(0.05 \times 126.9 \times 5) / 1000 = 0.03\text{g}$

Wt of LiI =  $(0.1 \times 133.85 \times 5) / 1000 = 0.066\text{g}$

Wt. of Imidazolium Cyanide =  $(0.6 \times 177.2 \times 5) / 1000 = 0.531\text{g}$

2.5ml of Acetonitrile

This solution was then stirred for 5-10 mins.

**C) PREPARING Pt. ELECTRODES:**

The Pt. electrodes were cleaned with acetonitrile because that has been used in the electrolyte.

After cleaning with acetonitrile, we sonicate it with DI water and successively with acetone for 10 mins each.

**D) TREATING THE ZnO FILMS WITH DYE:**

The ZnO films so formed on the FTO substrates were treated with the G1 dye using chemical bath deposition for 16 hours.

### PREPARING CELL:

Solar cell was then prepared by putting the FTO substrate(the side containing the film) and the Pt. electrodes over each other with the electrolyte in between. This cell was then clipped and connections were taken for Cell characteristic measurements.

The Cell Characteristics were measured using Cell Tester (Model No.-CT100AAA)

The various Cell characteristics measured are given below:

Sl no.	Sample name	V <sub>oc</sub>	Efficiency	FF
1	2	612.6mV	0.53%	0.557
2	3	259.4mV	0.28%	0.339
3	4	229.6	0.1%	0.278

Table 8

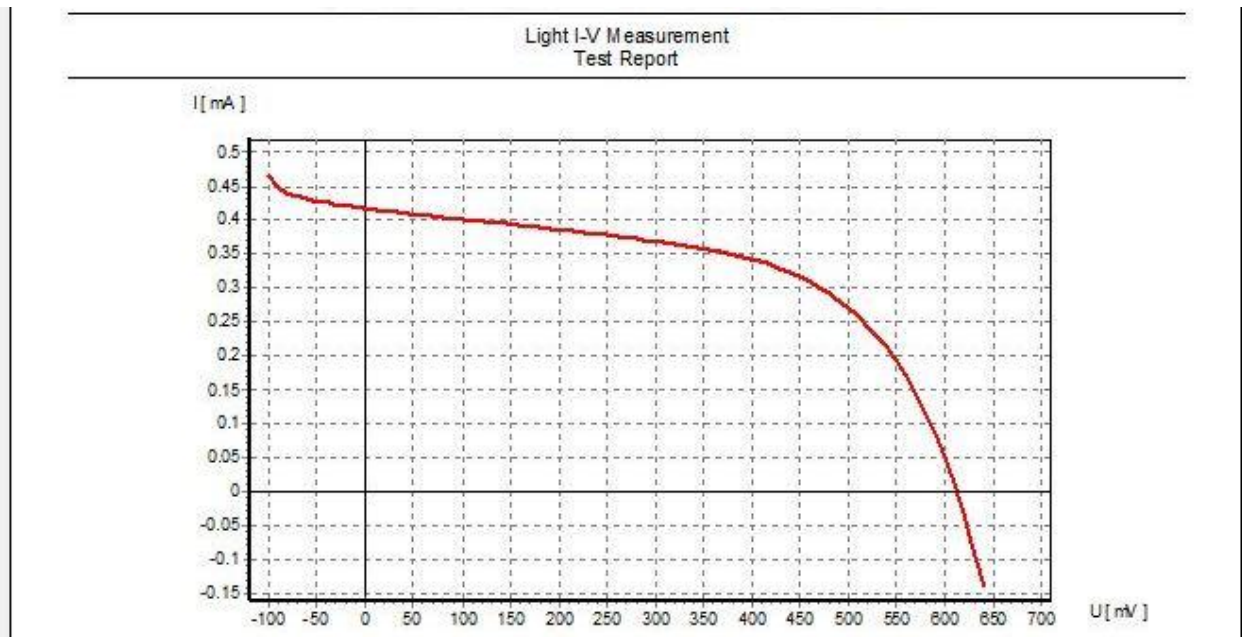


Figure 37 Fig showing I vs. V plot of cell 4.

The plots regarding J vs. V of these cells are given below:

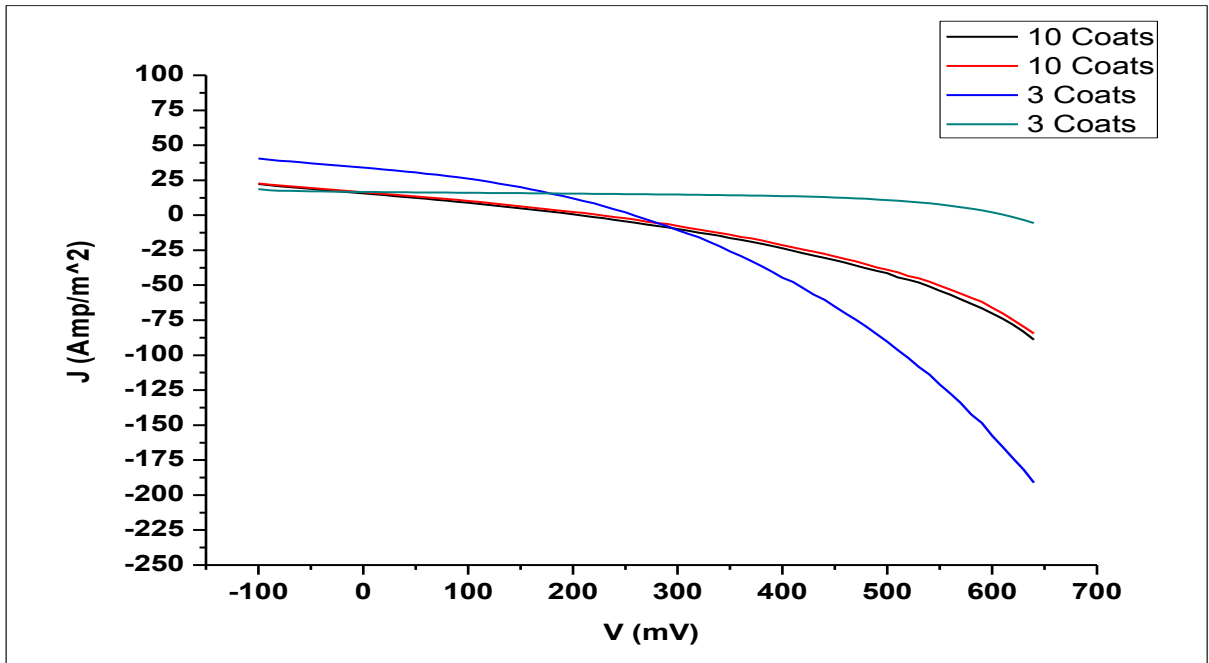


Figure 38 J vs. V of the DSSC's

## **7-CONCLUSION:**

ZnO being a semiconductor has a direct band gap of 3.4eV, thus making it capable of absorbing the UV wavelength of sunlight. Individually the dye G1 also has lower absorption power even though it can absorb the visible radiation of sunlight. But when ZnO is treated with G1, the absorption power gets considerably increased than their individual self thus making the thin film ideal for absorbing the visible radiation of sunlight. Also when tested with the cell tester (Model-CT100AAA), these DSSC reported a maximum  $V_{OC}$  of 612.6mV which is considerably quite good. For the inconsistency in the J vs. V curves of these DSSC, it may have happened that the electrolyte didn't cover the thin film fully which might have hampered in the electron injection or it may have happened because of any defect in the substrate.

## 8. References:

1. Segets, D.; Gradl, J.; Taylor, R.K.; Vassilev, V.; Peukert, W. Analysis of optical absorbance spectra for the determination of ZnO nanoparticle size distribution, solubility, and surface energy. *ACS Nano* **2009**, *3*, 1703–1710.
2. Lou, X. Development of ZnO series ceramic semiconductor gas sensors. *J. Sens. Trans. Technol.* **1991**, *3*, 1–5.
3. Bacaksiz, E.; Parlak, M.; Tomakin, M.; Özcelik, A.; Karakiz, M.; Altunbas, M. The effect of zinc nitrate, zinc acetate and zinc chloride precursors on investigation of structural and optical properties of ZnO thin films. *J. Alloy. Compd.* **2008**, *466*, 447–450.
4. Wang, J.; Cao, J.; Fang, B.; Lu, P.; Deng, S.; Wang, H. Synthesis and characterization of multipod, flower-like, and shuttle-like ZnO frameworks in ionic liquids. *Mater. Lett.* **2005**, *59*, 1405–1408.
5. Wang, Z.L. Splendid one-dimensional nanostructures of zinc oxide: A new nanomaterial family for nanotechnology. *ACS Nano* **2008**, *2*, 1987–1992.
6. Chaari, M.; Matoussi, A. Electrical conduction and dielectric studies of ZnO pellets. *Phys. B Condens. Matter* **2012**, *407*, 3441–3447.
7. Özgür, Ü.; Alivov, Y.I.; Liu, C.; Teke, A.; Reshchikov, M.A.; Doğan, S.; Avrutin, V.; Cho, S.J.; Morkoç, H. A comprehensive review of ZnO materials and devices. *J. Appl. Phys.* **2005**, *98*, doi:10.1063/1.1992666.
8. Bhattacharyya, S.; Gedanken, A. A template-free, sonochemical route to porous ZnO nano-disks. *Microporous Mesoporous Mater.* **2007**, *110*, 553–559.
9. Ludi, B.; Niederberger, M. Zinc oxide nanoparticles: Chemical mechanism and classical and non-classical crystallization. *Dalton Trans.* **2013**, *42*, 12554–12568.
10. Kandada, A. R. S., Guarnera, S., Tassone, F., Lanzani, G. and Petrozza, A. (2014), Charge Generation at Polymer/Metal Oxide Interface: from Molecular Scale Dynamics to Mesoscopic Effects. *Adv. Funct. Mater.*, *24*: 3094–3099. doi:10.1002/adfm.201303689
11. [https://en.wikipedia.org/wiki/Ultraviolet%E2%80%93visible\\_spectroscopy#/media/File:Schematic\\_of\\_UV-visible\\_spectrophotometer.png](https://en.wikipedia.org/wiki/Ultraviolet%E2%80%93visible_spectroscopy#/media/File:Schematic_of_UV-visible_spectrophotometer.png)



12. <http://energyprofessionalsymposium.com/?p=18499>
13. <http://www.pveducation.org/pvcdrom/solar-cell-operation/>
14. Simple fabrication process for 2D ZnO nanowalls and their potential application as a methane sensor. By Chen TP<sup>1</sup>, Chang SP, Hung FY, Chang SJ, Hu ZS, Chen KJ.
15. Zinc oxide nanostructures: growth, properties and applications by Zhong Lin Wang.
16. Optical and Luminescence Properties of Zinc Oxide P. A. Rodnyi and I. V. Khodyuk St. Petersburg State Technical University, St. Petersburg, 195251 Russia
17. Synthesis and Characterization of Zinc Oxide Nanoparticle by Sol-Gel Process by Surya Prakash Ghosh, Prof. Seemanchal Panigrahi
18. Training module # WQ – 34 on Absorption Spectroscopy
19. Dye-Sensitized Solar Cells Anders Hagfeldt, Gerrit Boschloo, Licheng Sun, Lars Kloo, and Henrik Pettersson
20. ZnO films prepared by modified sol – gel technique by R N Gayen, K Sarkar, S Hussain, A K Pal
21. Introduction to Photoluminescence Spectroscopy Lecturer: Shou-Yi Kuo
22. OPTICAL PROPERTIES OF ZnO NANOPARTICLES Soosen Samuel M, Lekshmi Bose and George KC
23. Absorption anisotropy studies of polymethine dyes Richard S. Lepkovicza, Claudiu M. Cirloganu, Olga V. Przhonska David J. Hagan, Eric W. Van Stryland, Mikhail V. Bondar Yuriy L. Slominsky, Alexei D. Kachkovski, Elena I. Mayboroda
24. The absorption spectrum, the signature of molecular motion LOS ALAMOS SCIENCE
25. Optical absorption edge of ZnO thin films: The effect of substrate V. Srikant and D. R. Clarke
26. Module 4 Atomic absorption Spectrometry by NPTEL
27. UV – Visible Spectrometry by NPTEL
28. Simple Preparation and Characterization of Nano-Crystalline Zinc Oxide Thin Films by Sol-Gel Method on Glass Substrate Muhammad Saleem, Liang Fang, Aneela Wakeel, M. Rashad, C. Y. Kong